Bulg. J. Phys. **45** (2018) 22–34

Symmetry-Based Approach to Shape Coexistence in Nuclei*

A. Leviatan, **N. Gavrielov**
Racah Institute of Physics, The Hebrew University, Jerusalem 91904, Israel

Received *7 January 2018*

Abstract. A symmetry-based approach for describing shape-coexistence, is presented in the framework of the interacting boson model of nuclei. It involves a construction of a number-conserving Hamiltonian which preserves the dynamical symmetry of selected bands associated with each shape, while breaking the symmetries in other states. The resulting structure embodies multiple partial dynamical symmetries. The procedure is applied to prolate-oblate and spherical-prolate-oblate coexistence, at and slightly away from the critical points.

PACS codes: 21.60.Fw, 21.10.Re, 21.60.Ev

1 Introduction

The presence of distinct shapes at similar low energies in a given nucleus, is a phenomena known to occur widely across the nuclear chart [1], including nuclei far from stability [2]. Notable empirical examples include the coexistence of prolate and oblate shapes in Kr [3], Se [4] and Hg isotopes [5], and the triple coexistence of spherical, prolate and oblate shapes in ^{186}Pb [6]. A detailed microscopic interpretation of nuclear shape-coexistence is a formidable task. In a shell model description of nuclei near shell-closure, it is attributed to the occurrence of multi-particle multi-hole intruder excitations across shell gaps. For medium-heavy nuclei, this necessitates drastic truncations of large model spaces, *e.g.*, by a bosonic approximation of nucleon pairs [7–13]. In a mean-field approach, based on energy density functionals, the coexisting shapes are associated with different minima of an energy surface calculated self-consistently. A detailed comparison with spectroscopic observables requires beyond mean-field methods, including restoration of broken symmetries and configuration mixing of angular-momentum and particle-number projected states [14, 15]. Such extensions present a major computational effort and often require simplifying assumptions such as a mapping to collective model Hamiltonians [16]. In the

*The article is based on a talk given at the International Workshop *Shapes and Dynamics of Atomic Nuclei: Contemporary Aspects* (SDANCA-17), 5–7 October 2017, Sofia, Bulgaria

present contribution, we consider a simple alternative to describe shape coexistence, in the framework of the interacting boson model (IBM) [17] of nuclei. The proposed approach is founded on the notion of partial dynamical symmetry (PDS) [18], emphasizing the role of remaining underlying symmetries which provide physical insight and make the problem tractable.

2 Dynamical Symmetries and Nuclear Shapes in the IBM

The IBM has been widely used to describe quadrupole collective states in nuclei in terms of N monopole ($s^\dagger$) and quadrupole ($d^\dagger$) bosons, representing valence nucleon pairs. The model has U(6) as a spectrum generating algebra and its solvable limits correspond to dynamical symmetries associated with the following chains of nested sub-algebras of U(6)

$$\mathrm{U}(6) \supset \mathrm{U}(5) \supset \mathrm{SO}(5) \supset \mathrm{SO}(3) \qquad |N,\, n_d,\, \tau,\, n_\Delta,\, L\rangle\,, \tag{1a}$$
$$\mathrm{U}(6) \supset \mathrm{SU}(3) \supset \mathrm{SO}(3) \qquad |N,\, (\lambda,\mu),\, K,\, L\rangle\,, \tag{1b}$$
$$\mathrm{U}(6) \supset \overline{\mathrm{SU}(3)} \supset \mathrm{SO}(3) \qquad |N,\, (\bar\lambda,\bar\mu),\, \bar K,\, L\rangle\,, \tag{1c}$$
$$\mathrm{U}(6) \supset \mathrm{SO}(6) \supset \mathrm{SO}(5) \supset \mathrm{SO}(3) \qquad |N,\, \sigma,\, \tau,\, n_\Delta,\, L\rangle\,. \tag{1d}$$

A dynamical symmetry (DS) occurs when the Hamiltonian is expressed in terms of the Casimir operators of a given chain, in which case, all states are solvable and classified by the indicated quantum numbers which are the labels of irreducible representations (irreps) of the algebras in the chain. The analytic solutions corresponding to the above DS chains, with leading subalgebras: U(5), SU(3), $\overline{\mathrm{SU}(3)}$ and SO(6), resemble known paradigms of nuclear collective structure: spherical vibrator, prolate-, oblate- and γ-soft deformed rotors, respectively. This identification is consistent with the geometric visualization of the model, obtained by an energy surface, $E_N(\beta,\gamma)$, defined by the expectation value of the Hamiltonian in the coherent (intrinsic) state [19, 20],

$$|\beta,\gamma;N\rangle = (N!)^{-1/2}(b_c^\dagger)^N\,|0\rangle\,, \tag{2a}$$
$$b_c^\dagger = (1+\beta^2)^{-1/2}[\beta\cos\gamma d_0^\dagger + \beta\sin\gamma(d_2^\dagger + d_{-2}^\dagger)/\sqrt{2} + s^\dagger]\,. \tag{2b}$$

Here (β,γ) are quadrupole shape parameters whose values, $(\beta_{\rm eq},\gamma_{\rm eq})$, at the global minimum of $E_N(\beta,\gamma)$ define the equilibrium shape for a given Hamiltonian. The equilibrium deformations associated with the DS limits conform with their geometric interpretation and are given by

$$\mathrm{U}(5): \qquad \beta_{\rm eq}=0 \qquad n_d=0\,, \tag{3a}$$
$$\mathrm{SU}(3): \qquad (\beta_{\rm eq}=\sqrt{2},\gamma_{\rm eq}=0) \qquad (\lambda,\mu)=(2N,0)\,, \tag{3b}$$
$$\overline{\mathrm{SU}(3)}: \qquad (\beta_{\rm eq}=\sqrt{2},\gamma_{\rm eq}=\pi/3) \qquad (\bar\lambda,\bar\mu)=(0,2N)\,, \tag{3c}$$
$$\mathrm{SO}(6): \qquad (\beta_{\rm eq}=1,\gamma_{\rm eq}\ \text{arbitrary}) \qquad \sigma=N\,. \tag{3d}$$

For these values, as shown, the equilibrium intrinsic state $|\beta_{\rm eq}, \gamma_{\rm eq}; N\rangle$ representing the ground band, becomes a lowest (or highest) weight state in a particular irrep of the leading sub-algebra in each of the chains of Eq. (1). The DS Hamiltonians support a single minimum in their energy surface, hence serve as benchmarks for the dynamics of a single quadrupole shape.

3 Partial Dynamical Symmetries and Shape Coexistence

A dynamical symmetry (DS) is characterized by *complete* solvability and good quantum numbers for *all* states. Often the symmetry in question is obeyed by only selected states, *e.g.* members of the ground band in deformed nuclei. The need to address such situations, but still preserve important symmetry remnants, has lead to the introduction of partial dynamical symmetry (PDS) [18, 21]. The latter is a generalization of the DS concept, and corresponds to a particular symmetry breaking for which only *some* of the states retain solvability and/or have good quantum numbers. In the present contribution, we show that this novel symmetry notion can play a vital role in formulating algebraic benchmarks for the dynamics of multiple quadrupole shapes. We focus on the dynamics in the vicinity of the critical point, where the corresponding multiple minima in the energy surface are near-degenerate and the structure changes most rapidly.

Consider one of the DS chains of Eq. (1),

$$\mathrm{U}(6) \supset \mathrm{G}_1 \supset \mathrm{G}_2 \supset \ldots \supset \mathrm{SO}(3) \qquad |N,\, \lambda_1,\, \lambda_2,\, \ldots,\, L\rangle\,, \tag{4}$$

with leading sub-algebra G_1, related basis and associated shape $(\beta_{\rm eq}, \gamma_{\rm eq})$. The construction of an Hamiltonian with PDS is done by requiring it to satisfy

$$\hat{H}|\beta_{\rm eq}, \gamma_{\rm eq}; N, \lambda_1 = \Lambda_0, \lambda_2, \ldots, L\rangle = 0\,. \tag{5}$$

The set of zero-energy eigenstates in Eq. (5) are basis states of a particular G_1-irrep, $\lambda_1 = \Lambda_0$, and have good G_1 symmetry. For a positive-definite $\hat{H}$, they span the ground band of the equilibrium shape and can be obtained by L-projection from the corresponding intrinsic state, $|\beta_{\rm eq}, \gamma_{\rm eq}; N\rangle$ of Eq. (2). $\hat{H}$ itself, however, need not be invariant under G_1 and, therefore, has partial-G_1 symmetry. The Hamiltonian of Eq. (5) serves as the intrinsic part of the complete Hamiltonian, $\hat{H}' = \hat{H} + \hat{H}_c$. Identifying the collective part ($\hat{H}_c$) with the Casimir operators of the remaining sub-algebras of G_1 in the chain (4), the degeneracy of the above set of states is lifted, and they remain solvable eigenstates of $\hat{H}'$. The latter, by definition, has G_1-PDS and exemplifies an intrinsic-collective resolution [22–25], where the intrinsic part ($\hat{H}$) determines the energy surface, and the collective part ($\hat{H}_c$) is composed of kinetic rotational terms. IBM Hamiltonians with a single PDS, constructed in this manner, have been shown to be relevant to a broad range of nuclei with a single quadrupole shape [26–34].

Coexistence of distinct shapes in the same nucleus, arises from competing terms in the Hamiltonian whose energy surface exhibits multiple minima, with different types of dynamics (and symmetry) associated with each minimum. In such circumstances, exact DSs are broken, and remaining symmetries, if any, are at most partial. A symmetry-based approach thus requires an extension of the above procedure to encompass a construction of Hamiltonians with several distinct PDSs [35–38]. For that purpose, consider two different shapes specified by equilibrium deformations (β_1, γ_1) and (β_2, γ_2) whose dynamics is described, respectively, by the following DS chains

$$\mathrm{U}(6) \supset \mathrm{G}_1 \supset \mathrm{G}_2 \supset \ldots \supset \mathrm{SO}(3) \qquad |N,\, \lambda_1,\, \lambda_2,\, \ldots,\, L\rangle\,, \tag{6a}$$

$$\mathrm{U}(6) \supset \mathrm{G}'_1 \supset \mathrm{G}'_2 \supset \ldots \supset \mathrm{SO}(3) \qquad |N,\, \sigma_1,\, \sigma_2,\, \ldots,\, L\rangle\,, \tag{6b}$$

with different leading sub-algebras ($G_1 \neq G'_1$) and associated bases. At the critical point, the corresponding minima representing the two shapes and the respective ground bands are degenerate. Accordingly, we require the intrinsic critical-point Hamiltonian to satisfy simultaneously the following two conditions

$$\hat{H}|\beta_1, \gamma_1; N, \lambda_1 = \Lambda_0, \lambda_2, \ldots, L\rangle = 0\,, \tag{7a}$$

$$\hat{H}|\beta_2, \gamma_2; N, \sigma_1 = \Sigma_0, \sigma_2, \ldots, L\rangle = 0\,. \tag{7b}$$

The states of Eq. (7a) reside in the $\lambda_1 = \Lambda_0$ irrep of G_1, are classified according to the DS-chain (6a), hence have good G_1 symmetry. Similarly, the states of Eq. (7b) reside in the $\sigma_1 = \Sigma_0$ irrep of G'_1, are classified according to the DS-chain (6b), hence have good G'_1 symmetry. Although G_1 and G'_1 are incompatible (non-commuting) symmetries, both sets are eigenstates of the same Hamiltonian. When the latter is positive definite, the two sets span the ground bands of the (β_1, γ_1) and (β_2, γ_2) shapes, respectively. In general, $\hat{H}$ itself is not necessarily invariant under G_1 nor under G_2 and, therefore, its other eigenstates can be mixed under both G_1 and G'_1. Identifying the collective part of the Hamiltonian with the Casimir operator of SO(3) (as well as with the Casimir operators of additional algebras which are common to both chains), the two sets of states remain (non-degenerate) eigenstates of the complete Hamiltonian which then has both G_1-PDS and G'_1-PDS. The case of triple (or multiple) shape coexistence, associated with three (or more) incompatible DS-chains is treated in a similar fashion.

The solution of Eqs. (7), if exists, results in a single number-conserving, rotational-invariant Hamiltonian with, possibly, higher-order terms. The effective Hamiltonian constructed in this manner, conserves the multiple DSs but only in selected bands. This strategy is different from that used in the IBM with configuration mixing [7–10], where shape coexistence is described by different Hamiltonians for the normal and intruder configurations and a number-non-conserving mixing term. In what follows, we apply the above procedure to

a case study of double- and triple coexistence of prolate-oblate and spherical-prolate-oblate shapes.

4 Prolate-Oblate and Spherical-Prolate-Oblate Shape Coexistence

The DS limits appropriate to prolate and oblate shapes correspond to the chains (1b) and (1c), respectively. For a given U(6) irrep N, the allowed SU(3) [$\overline{\mathrm{SU}(3)}$] irreps are $(\lambda,\mu)=(2N-4k-6m,2k)$ [$(\bar\lambda,\bar\mu)=(2k,2N-4k-6m)$] with k,m, non-negative integers. The multiplicity label K ($\bar K$) corresponds geometrically to the projection of the angular momentum (L) on the symmetry axis. The basis states are eigenstates of the Casimir operator $\hat C_2[\mathrm{SU}(3)]$ or $\hat C_2[\overline{\mathrm{SU}(3)}]$, where $\hat C_k[G]$ denotes the Casimir operator of G of order k. Specifically, $\hat C_2[\mathrm{SU}(3)]=2Q^{(2)}\cdot Q^{(2)}+\frac{3}{4}L^{(1)}\cdot L^{(1)}$, $Q^{(2)}=d^\dagger s+s^\dagger\tilde d-\frac{1}{2}\sqrt{7}(d^\dagger\tilde d)^{(2)}$, $L^{(1)}=\sqrt{10}(d^\dagger\tilde d)^{(1)}$, $\tilde d_\mu=(-1)^\mu d_{-\mu}$ and $\hat C_2[\overline{\mathrm{SU}(3)}]$ is obtained by replacing $Q^{(2)}$ by $\bar Q^{(2)}=d^\dagger s+s^\dagger\tilde d+\frac{1}{2}\sqrt{7}(d^\dagger\tilde d)^{(2)}$. The generators of SU(3) and $\overline{\mathrm{SU}(3)}$, $Q^{(2)}$ and $\bar Q^{(2)}$, and corresponding basis states, are related by a change of phase $(s^\dagger,s)\to(-s^\dagger,-s)$, induced by the operator $\mathcal{R}_s=\exp(i\pi\hat n_s)$, with $\hat n_s=s^\dagger s$. The DS Hamiltonian involves a linear combination of the Casimir operators in a given chain. The spectrum resembles that of an axially-deformed rotovibrator composed of SU(3) [or $\overline{\mathrm{SU}(3)}$] multiplets forming rotational bands, with $L(L+1)$-splitting generated by $\hat C_2[\mathrm{SO}(3)]=L^{(1)}\cdot L^{(1)}$. In the SU(3) [or $\overline{\mathrm{SU}(3)}$] DS limit, the lowest irrep $(2N,0)$ [or $(0,2N)$] contains the ground band $g(K=0)$ [or $g(\bar K=0)$] of a prolate [oblate] deformed nucleus. The first excited irrep $(2N-4,2)$ [or $(2,2N-4)$] contains both the $\beta(K=0)$ and $\gamma(K=2)$ [or $\beta(\bar K=0)$ and $\gamma(\bar K=2)$] bands. Henceforth, we denote such prolate and oblate bands by (g_1,β_1,γ_1) and (g_2,β_2,γ_2), respectively. Since $\mathcal{R}_sQ^{(2)}\mathcal{R}_s^{-1}=-\bar Q^{(2)}$, the SU(3) and $\overline{\mathrm{SU}(3)}$ DS spectra are identical and the quadrupole moments of corresponding states differ in sign.

The U(5)-DS limit of Eq. (1a) is appropriate to the dynamics of a spherical shape. For a given N, the allowed U(5) and SO(5) irreps are $n_d=0,1,2,\ldots,N$ and $\tau=n_d,\ n_d-2,\ldots 0$ or 1, respectively. The U(5)-DS spectrum resembles that of an anharmonic spherical vibrator, composed of U(5) n_d-multiplets whose spacing is governed by $\hat C_1[\mathrm{U}(5)]=\hat n_d=\sum_\mu d_\mu^\dagger d_\mu$, and splitting is generated by the SO(5) and SO(3) terms. The lowest U(5) multiplets involve the ground state with quantum numbers $(n_d=0,\ \tau=0,\ L=0)$ and excited states with quantum numbers $(n_d=1,\ \tau=1,\ L=2)$ and $(n_d=2:\ \tau=0,\ L=0;\ \tau=2,\ L=2,4)$.

Following the procedure of Eq. (7), the intrinsic part of the critical-point Hamiltonian, relevant to prolate-oblate (P-O) coexistence, is required to satisfy

$$\hat H|N,\ (\lambda,\mu)=(2N,0),\ K=0,\ L\rangle=0\ , \tag{8a}$$

$$\hat H|N,\ (\bar\lambda,\bar\mu)=(0,2N),\ \bar K=0,\ L\rangle=0\ . \tag{8b}$$

Equivalently, $\hat H$ annihilates the intrinsic states of Eq. (2), with $(\beta=\sqrt{2},\gamma=0)$

and $(\beta = -\sqrt{2}, \gamma = 0)$, which are the lowest- and highest-weight vectors in the irreps $(2N, 0)$ and $(0, 2N)$ of SU(3) and $\overline{\mathrm{SU}(3)}$, respectively. The resulting Hamiltonian is found to be [37],

$$\hat{H} = h_0\, P_0^\dagger \hat{n}_s P_0 + h_2\, P_0^\dagger \hat{n}_d P_0 + \eta_3\, G_3^\dagger \cdot \tilde{G}_3\ , \tag{9}$$

where $P_0^\dagger = d^\dagger \cdot d^\dagger - 2(s^\dagger)^2$, $G^\dagger_{3,\mu} = \sqrt{7}[(d^\dagger d^\dagger)^{(2)} d^\dagger]^{(3)}_\mu$, $\tilde{G}_{3,\mu} = (-1)^\mu G_{3,-\mu}$ and the centered dot denotes a scalar product. The corresponding energy surface, $E_N(\beta,\gamma) = N(N-1)(N-2)\tilde{E}(\beta,\gamma)$, is given by

$$\tilde{E}(\beta,\gamma) = \left\{(\beta^2-2)^2\left[h_0 + h_2\beta^2\right] + \eta_3\beta^6\sin^2(3\gamma)\right\}(1+\beta^2)^{-3}\ . \tag{10}$$

The surface is an even function of β and $\Gamma = \cos 3\gamma$, and can be transcribed as $\tilde{E}(\beta,\gamma) = z_0 + (1+\beta^2)^{-3}[A\beta^6 + B\beta^6\Gamma^2 + D\beta^4 + F\beta^2]$, with $A = -4h_0 + h_2 + \eta_3$, $B = -\eta_3$, $D = -(11h_0 + 4h_2)$, $F = 4(h_2 - 4h_0)$, $z_0 = 4h_0$. For $h_0, h_2, \eta_3 \geq 0$, $\hat{H}$ is positive definite and $\tilde{E}(\beta,\gamma)$ has two degenerate global minima, $(\beta = \sqrt{2}, \gamma = 0)$ and $(\beta = \sqrt{2}, \gamma = \pi/3)$ [or equivalently $(\beta = -\sqrt{2}, \gamma = 0)$], at $\tilde{E} = 0$. $\beta = 0$ is always an extremum, which is a local minimum (maximum) for $F > 0$ ($F < 0$), at $\tilde{E} = 4h_0$. Additional extremal points include saddle points at $[\beta_1 > 0, \gamma = 0, \pi/3]$, $[\beta_2 > 0, \gamma = \pi/6]$ and a local maximum at $[\beta_3 > 0, \gamma = \pi/6]$. The saddle points, when exist, support a barrier separating the various minima, as seen in Figure 1. For large N, the normal modes involve β and γ vibrations about the respective deformed minima, with frequencies

$$\epsilon_{\beta 1} = \epsilon_{\beta 2} = \frac{8}{3}(h_0 + 2h_2)N^2\ , \tag{11a}$$

$$\epsilon_{\gamma 1} = \epsilon_{\gamma 2} = 4\eta_3 N^2\ . \tag{11b}$$

For $h_0 = 0$, also $\beta = 0$ becomes a global minimum, resulting in three degenerate minima corresponding to coexistence of prolate, oblate and spherical (S-P-O) shapes. $\hat{H}(h_0 = 0)$ satisfies Eq. (8) and has also the following U(5) basis state

$$\hat{H}(h_0 = 0)|N, n_d = \tau = L = 0\rangle = 0\ , \tag{12}$$

as an eigenstate. Equivalently, it annihilates the intrinsic state of Eq. (2), with $\beta = 0$. The additional normal modes involve quadrupole vibrations about the spherical minimum, with frequency

$$\epsilon = 4h_2 N^2\ . \tag{13}$$

The members of the prolate and oblate ground-bands, Eq. (8), are zero-energy eigenstates of $\hat{H}$ (9), with good SU(3) and $\overline{\mathrm{SU}(3)}$ symmetry, respectively. The Hamiltonian is invariant under a change of sign of the s-bosons, hence commutes with the $\mathcal{R}_s$ operator mentioned above. Consequently, all non-degenerate eigenstates of $\hat{H}$ have well-defined s-parity. This implies vanishing quadrupole moments for an $E2$ operator which is odd under such sign

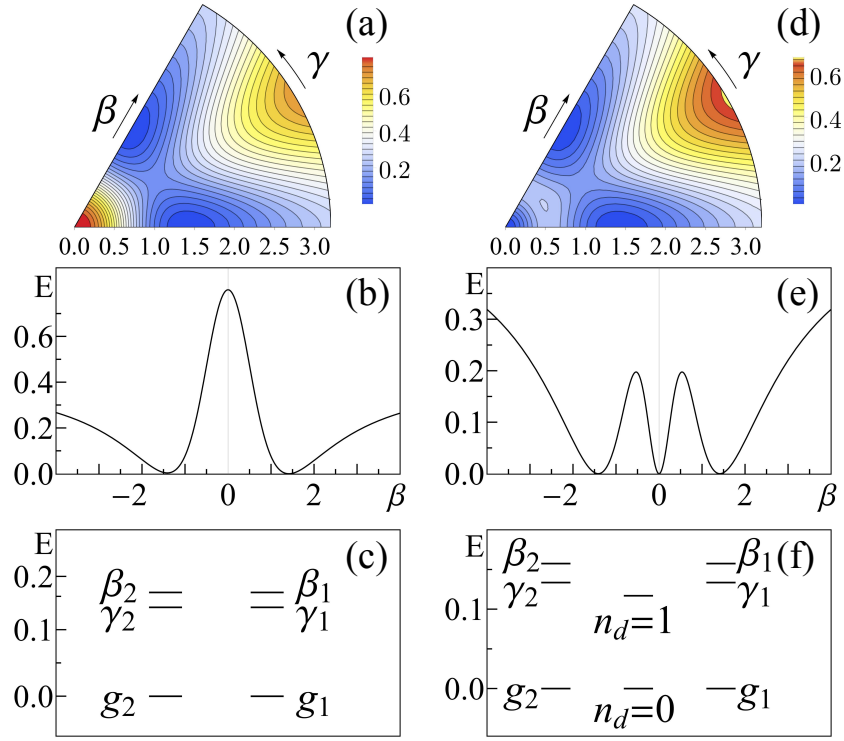

Figure 1. (Color online) Contour plots of the energy surface (10) [top row], $\gamma=0$ sections [middle row] and bandhead spectrum [bottom row] for the Hamiltonian (14), with $\alpha=0.018$, $\eta_3=0.571$, $\rho=0$, $N=20$. Panels (a)-(b)-(c) [(d)-(e)-(f)] correspond to the choice $h_0=0.2$, $h_2=0.4$ [$h_0=0$, $h_2=0.5$] resulting in prolate-oblate [spherical-prolate-oblate] shape coexistence.

change. To overcome this difficulty, we introduce a small s-parity breaking term $\alpha\hat{\theta}_2=\alpha[-\hat{C}_2[SU(3)]+2\hat{N}(2\hat{N}+3)]$, which contributes to $\tilde{E}(\beta,\gamma)$ a component $\tilde{\alpha}(1+\beta^2)^{-2}[(\beta^2-2)^2+2\beta^2(2-2\sqrt{2}\beta\Gamma+\beta^2)]$, with $\tilde{\alpha}=\alpha/(N-2)$. The linear Γ-dependence distinguishes the two deformed minima and slightly lifts their degeneracy, as well as that of the normal modes (11). Replacing $\hat{\theta}_2$ by $\bar{\theta}_2=-\hat{C}_2[\overline{\mathrm{SU}(3)}]+2\hat{N}(2\hat{N}+3)$, leads to similar effects but interchanges the role of prolate and oblate bands. Identifying the collective part with $\hat{C}_2[\mathrm{SO}(3)]$, we arrive at the following complete Hamiltonian

$$\hat{H}'=h_0\,P_0^\dagger\hat{n}_sP_0+h_2\,P_0^\dagger\hat{n}_dP_0+\eta_3\,G_3^\dagger\cdot\tilde{G}_3+\alpha\,\hat{\theta}_2+\rho\,\hat{C}_2[\mathrm{SO}(3)]\ . \quad (14)$$

Figures 1(a)-1(b)-1(c) [1(d)-1(e)-1(f)] show $\tilde{E}(\beta,\gamma)$, $\tilde{E}(\beta,\gamma=0)$ and the bandhead spectrum of $\hat{H}'$ (14), with parameters ensuring degenerate P-O [S-

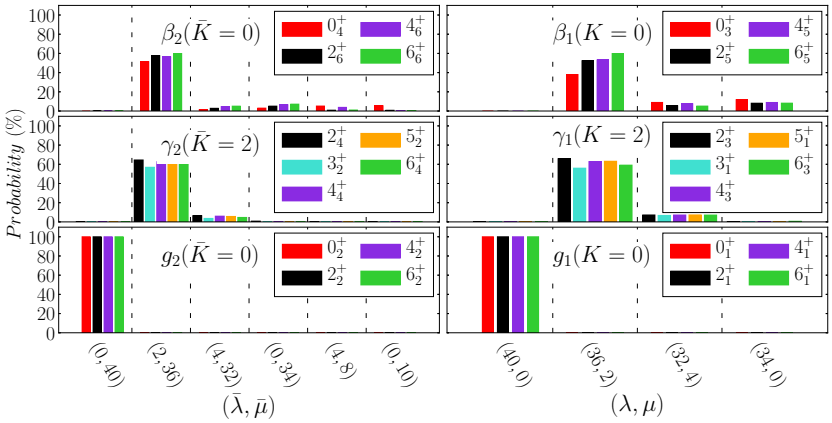

Figure 2. (Color online) SU(3) (λ,μ)- and $\overline{\mathrm{SU}(3)}$ $(\bar{\lambda},\bar{\mu})$-decompositions for members of the prolate (g_1,β_1,γ_1) and oblate (g_2,β_2,γ_2) bands, eigenstates of $\hat{H}'$ (14) with parameters as in Figure 1(c), resulting in prolate-oblate (P-O) shape coexistence. Shown are probabilities larger than 5%.

P-O] minima. The prolate g_1-band remains solvable with energy $E_{g1}(L) = \rho L(L+1)$. The oblate g_2-band experiences a slight shift of order $\frac{32}{9}\alpha N^2$ and displays a rigid-rotor like spectrum. In the case of P-O coexistence, the SU(3) and $\overline{\mathrm{SU}(3)}$ decomposition in Figure 2 demonstrates that these bands are pure DS basis states, with $(2N,0)$ and $(0,2N)$ character, respectively, while excited β and γ bands exhibit considerable mixing. The critical-point Hamiltonian thus

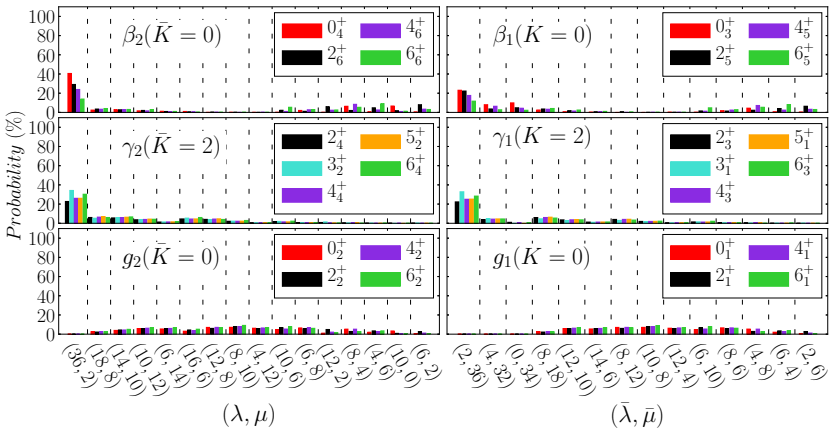

Figure 3. (Color online) As in Figure 2, but now states of the prolate (g_1,β_1,γ_1) bands are expanded in the $\overline{\mathrm{SU}(3)}$ basis, while states of the oblate (g_2,β_2,γ_2) bands are expanded in the SU(3) basis. Shown are probabilities larger than 6%.

has a subset of states with good SU(3) symmetry, a subset of states with good $\overline{\mathrm{SU}(3)}$ symmetry and all other states are mixed with respect to both SU(3) and $\overline{\mathrm{SU}(3)}$. These are precisely the defining ingredients of SU(3)-PDS coexisting with $\overline{\mathrm{SU}(3)}$-PDS. The two persisting symmetries are incompatible, as is evident from Figure 3, where the same prolate (g_1, β_1, γ_1) bands are expanded in the $\overline{\mathrm{SU}(3)}$ basis, while the oblate (g_2, β_2, γ_2) bands are expanded in the SU(3) basis. All states, including the solvable ones, are seen to be strongly mixed and highly fragmented among many irreps.

In the case of triple S-P-O coexistence, the prolate and oblate bands show similar behaviour. A new aspect is the simultaneous occurrence in the spectrum [Figure 1(f)] of spherical type of states, whose wave functions are dominated by a single n_d component. As shown in Figure 4, the lowest spherical states have quantum numbers $(n_d = L = 0)$ and $(n_d = 1, L = 2)$, hence coincide with pure U(5) basis states, while higher spherical states have a pronounced ($\sim$70%) $n_d = 2$ component. This structure should be contrasted with the U(5) decomposition of deformed states (belonging to the g_1 and g_2 bands) which, as shown in Figure 4, have a broad n_d-distribution. The purity of selected sets of states with respect to SU(3), $\overline{\mathrm{SU}(3)}$ and U(5), in the presence of other mixed states, are the hallmarks of coexisting partial dynamical symmetries.

Since the wave functions for the members of the g_1 and g_2 bands are known, one can derive analytic expressions for their quadrupole moments and $E2$ transition rates. Considering the $E2$ operator $T(E2) = e_B\, \Pi^{(2)}$ with

$$\Pi^{(2)} = d^\dagger s + s^\dagger \tilde{d}\,, \tag{15}$$

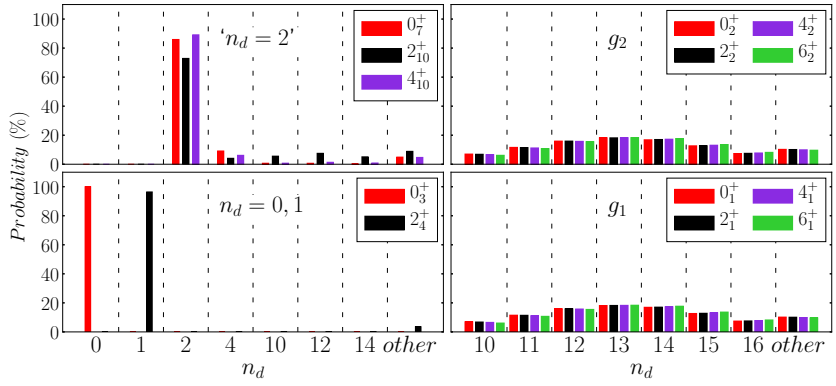

Figure 4. (Color online) U(5) n_d-decomposition for spherical states (left panels) and for members of the deformed prolate (g_1) and oblate (g_2) ground bands (right panels), eigenstates of $\hat{H}'$ (14) with parameters as in Figure 1(f), resulting in spherical-prolate-oblate (S-P-O) shape coexistence. The column 'other' depicts a sum of probabilities, each less than 5%.

the quadrupole moments are found to have equal magnitudes and opposite signs,

$$Q_L = \mp e_B \sqrt{\frac{16\pi}{40}} \frac{L}{2L+3} \frac{4(2N-L)(2N+L+1)}{3(2N-1)} \,, \tag{16}$$

where the minus (plus) sign corresponds to the prolate-g_1 (oblate-g_2) band. The $B(E2)$ values for intraband ($g_1 \to g_1$, $g_2 \to g_2$) transitions,

$$B(E2; g_i,\, L+2 \to g_i,\, L) = \\ e_B^2 \, \frac{3(L+1)(L+2)}{2(2L+3)(2L+5)} \frac{(4N-1)^2(2N-L)(2N+L+3)}{18(2N-1)^2} \,, \tag{17}$$

are the same. These properties are ensured by the fact that $\mathcal{R}_s T(E2) \mathcal{R}_s^{-1} = -T(E2)$. Interband ($g_2 \leftrightarrow g_1$) $E2$ transitions, are extremely weak. This follows from the fact that the L-states of the g_1 and g_2 bands exhaust, respectively, the $(2N,0)$ and $(0,2N)$ irrep of SU(3) and $\overline{\mathrm{SU}(3)}$. $T(E2)$ contains a $(2,2)$ tensor under both algebras, hence can connect the $(2N,0)$ irrep of g_1 only with the $(2N-4,2)$ component in g_2 which, as seen in Figure 3, is vanishingly small. The selection rule $g_1 \nleftrightarrow g_2$ is valid also for a more general $E2$ operator, obtained by including in it the operators $Q^{(2)}$ or $\bar{Q}^{(2)}$, since the latter, as generators, cannot mix different irreps of SU(3) or $\overline{\mathrm{SU}(3)}$. By similar arguments, $E0$ transitions in-between the g_1 and g_2 bands are extremely weak, since the relevant operator, $T(E0) \propto \hat{n}_d$, is a combination of $(0,0)$ and $(2,2)$ tensors under both algebras. In contrast to g_1 and g_2, excited β and γ bands are mixed, hence are connected by $E2$ transitions to these ground bands.

In the case of triple (S-P-O) coexistence, since $T(E2)$ obeys the selection rule $\Delta n_d = \pm 1$, the spherical states, $(n_d = L = 0)$ and $(n_d = 1, L = 2)$, have no quadrupole moment and the B($E2$) value for their connecting transition, obeys the U(5)-DS expression [17]

$$B(E2; n_d = 1, L = 2 \to n_d = 0, L = 0) = e_B^2 N \,. \tag{18}$$

These spherical states have very weak $E2$ transitions to the deformed ground bands, because they exhaust the $(n_d = 0, 1)$ irreps of U(5), and the $n_d = 2$ component in the ($L = 0, 2, 4$) states of the g_1 and g_2 bands is extremely small, of order $N^3 3^{-N}$, as seen in Figure 4. There are also no $E0$ transitions involving these spherical states, since $T(E0)$ is diagonal in n_d. The analytic expressions of Eqs. (16)-(18) are parameter-free predictions, except for a scale, and can be used to compare with measured values of these observables and to test the underlying SU(3), $\overline{\mathrm{SU}(3)}$ and U(5) partial symmetries.

The above discussion has focused on the dynamics in the vicinity of the critical point where the multiple minima are near degenerate. The evolution of structure away from the critical point, can be studied by varying the coupling constants or by incorporating additional terms in $\hat{H}'$ (14). In case of P-O coexistence,

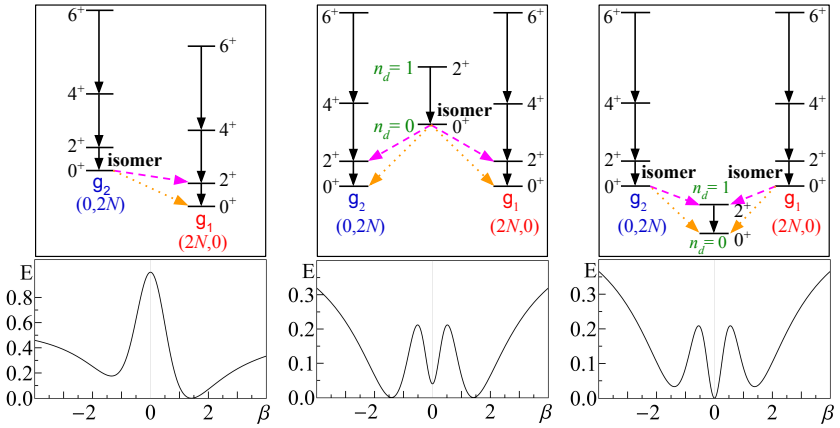

Figure 5. (Color online) Energy-surface sections and level schemes corresponding to departures from the critical point for $\hat{H}'$, Eq. (14), with $\eta_3 = 0.571$, $\rho = 1$ and $N = 20$. Left panels: P-O coexistence, oblate isomeric state ($h_0 = 0.2$, $h_2 = 0.4$, $\alpha = 0.9$). Middle panels: S-P-O coexistence, a spherical isomeric state ($h_0 = 0.01$, $h_2 = 0.5$, $\alpha = 0.018$). Right panels: S-P-O coexistence, deformed isomeric states ($h_0 = 0$, $h_2 = 0.5$, $\alpha = 0.018$ and an added $\epsilon \hat{n}_d$ term with $\epsilon = 10$). Retarded $E2$ (dashes lines) and $E0$ (dotted lines) decays identify the isomeric states.

taking larger values of α, will leave the prolate g_1-band unchanged, but will shift the oblate g_2-band to higher energy of order $16\alpha N^2/9$. In case of triple S-P-O coexistence, if the spherical minimum is only local, one can use $\hat{H}'$ (14) with parameters satisfying $h_2 > 4h_0$, for which the spherical ground state ($n_d = L = 0$) experiences a shift of order $4h_0N^3$, but the deformed ground bands are unchanged. Otherwise, if the deformed minima are only local, adding an $\epsilon \hat{n}_d$ term to $\hat{H}'(h_0 = 0)$ will leave the $n_d = 0$ spherical ground state unchanged, but will shift the prolate and oblate bands to higher energy of order $2\epsilon N/3$. The resulting topology of the energy surfaces with such modifications are shown at the bottom row of Figure 5. If these departures from the critical points are small, the wave functions decomposition of Figures 2-4 remain intact and the analytic expressions for E2 observables and selection rules are still valid to a good approximation. In such scenarios, the lowest $L = 0$ state of the non-yrast configuration will exhibit retarded $E2$ and $E0$ decays, hence will have the attributes of an isomer state, as depicted schematically on the top row of Figure 5.

Acknowledgments

This work is supported by the Israel Science Foundation (Grant 586/16).

References

[1] K. Heyde and J.L. Wood (2011) *Rev. Mod. Phys.* **83** 1467.

[2] D.G. Jenkins (2014) *Nature Phys* **10** 909.

[3] E. Clément *et al.* (2007) *Phys. Rev. C* **75** 054313.

[4] J. Ljungvall *et al.* (2008) *Phys. Rev. Lett.* **100** 102502.

[5] N. Bree *et al.* (2014) *Phys. Rev. Lett.* **112** 162701.

[6] A.N. Andreyev *et al.* (2000) *Nature* **405** 430.

[7] P.D. Duval and B.R. Barrett (1981) *Phys. Lett. B* **100** 223.

[8] R. Fossion, K. Heyde, G. Thiamova and P. Van Isacker (2003) *Phys. Rev. C* **67** 024306.

[9] A. Frank A, P. Van Isacker P and C.E. Vargas (2004) *Phys. Rev. C* **69** 034323.

[10] I.O. Morales, A. Frank, C.E. Vargas and P. Van Isacker (2008) *Phys. Rev. C* **78** 024303.

[11] J.E. García-Ramos and K. Heyde (2014) *Phys. Rev. C* **89** 014306.

[12] K. Nomura, R. Rodríguez-Guzmán, L.M. Robledo (2013) *Phys. Rev. C* **87** 064313.

[13] K. Nomura, T. Otsuka and P. Van Isacker (2016) *J. Phys. G* **43** 024008.

[14] J.M. Yao, M. Bender and P.-H. Heenen (2013) *Phys. Rev. C* **87** 034322.

[15] Z.P. Li, T. Nikšić and D. Vretenar (2016) *J. Phys. G* **43** 024005.

[16] K. Nomura, T. Nikšić, T. Otsuka, N. Shimizu and D. Vretenar (2011) *Phys. Rev. C* **84** 014302

[17] F. Iachello and A. Arima (1987) *The Interacting Boson Model*, Cambridge University Press, Cambridge.

[18] A. Leviatan (2011) *Prog. Part. Nucl. Phys.* **66** 93.

[19] J.N. Ginocchio and M.W. Kirson (1980) *Phys. Rev. Lett.* **44** 1744.

[20] A.E.L. Dieperink, O. Scholten and F. Iachello (1980) *Phys. Rev. Lett.* **44** 1747.

[21] Y. Alhassid and A. Leviatan (1992) *J. Phys. A* **25** L1265.

[22] M.W. Kirson and A. Leviatan (1985) *Phys. Rev. Lett.* **55** 2846.

[23] A. Leviatan (1987) *Ann. Phys. (N.Y.)* **179** 201.

[24] A. Leviatan and M.W. Kirson (1990) *Ann. Phys. (N.Y.)* **201** 13.

[25] A. Leviatan (2006) *Phys. Rev. C* **74** 051301(R).

[26] A. Leviatan (1996) *Phys. Rev. Lett.* **77** 818.

[27] A. Leviatan and I. Sinai (1999) *Phys. Rev. C* **60** 061301(R).

[28] R. F. Casten, R. B. Cakirli, K. Blaum and A. Couture (2014) *Phys. Rev. Lett.* **113** 112501.

[29] A. Couture, R. F. Casten and R. B. Cakirli (2015) *Phys. Rev. C* **91** 014312.

[30] J. E. García-Ramos, A. Leviatan and P. Van Isacker (2009) *Phys. Rev. Lett.* **102** 112502.

[31] A. Leviatan, J. E. García-Ramos, and P. Van Isacker (2013) *Phys. Rev. C* **87** 021302(R).

[32] C. Kremer, J. Beller, A. Leviatan, N. Pietralla, G. Rainovski, R. Trippel, and P. Van Isacker (2014) *Phys. Rev. C* **89**, 041302(R); (2015) *Phys. Rev. C* **92** 039902.

[33] A. Leviatan and J.N. Ginocchio (2000) *Phys. Rev. C* **61** 024305.

[34] P. Van Isacker, J. Jolie, T. Thomas and A. Leviatan (2015) *Phys. Rev. C* **92** 011301(R).
[35] A. Leviatan (2007) *Phys. Rev. Lett.* **98** 242502.
[36] M. Macek and A. Leviatan (2014) *Ann. Phys. (N.Y.)* **351** 302.
[37] A. Leviatan and D. Shapira (2016) *Phys. Rev. C* **93** 051302(R).
[38] A. Leviatan and N. Gavrielov (2017) *Phys. Scr.* **92** 114005.